Proceedings of the 37th IAHR World Congress
August 13 – 18, 2017, Kuala Lumpur, Malaysia

INFLUENCE OF LATERAL RECTANGULAR EMBAYMENTS ON THE TRANSPORT OF SUSPENDED SEDIMENTS IN A FLUME

CARMELO JUEZ[1], IRIA BUEHLMANN[2], GAETAN MAECHLER[3], ANTON J. SCHLEISS[4] & MÁRIO J. FRANCA[5]

[1,2,3,4,5] École Polytechnique Fédéral de Lausanne (EPFL), Lausanne, Switzerland
carmelo.juez@epfl.ch

ABSTRACT

Systematic experimental investigations have been performed under uniform flow conditions in a channel whose banks are equipped with large scale rectangular roughness elements. The practical motivation of this project is to see how restoration of banks, such as lateral cavities, has an influence on the transport of fine sediments. The implementation of lateral cavities may affect the sediment and morphological equilibrium of the river since these may trap sediments. This work aims to study the influence of the lateral cavities on the transport of fine sediments in the main channel. A set of laboratory experiments are done which covers a wide range of rectangular cavity configurations and includes aspect ratios (lateral cavity depth divided by cavity length) between 0.2 and 0.8. Key parameters such as the flow discharge and the initial sediment concentration are tested. Surface PIV, sediment samples and turbidity temporal records are collected during the experiments. The trapping efficiency of the cavities and the associated flow patterns are calculated and discussed. The resulting conclusions provide useful information for the future design of river restoration projects.

Keywords: Fine sediments; river restoration; ateral embayments; surface PIV; shallow flows.

1 INTRODUCTION

River restoration is nowadays a major issue in the field of hydraulics. The natural course and geometry of the rivers have been artificially changed by human activities for different purposes (land gaining, flood protection, agriculture, hydropower production). However, this man intervention has caused an alteration in the continuity of the sediment transport (Allan and Castillo, 2007; Schleiss et al., 2016). This way, the quasi-natural equilibrium between the in-coming and outgoing fluxes of sediments is broken (McCartney, 2009), leading to: (i) a deficit situation or (ii) an excess situation downstream the reaches with a deficit situation. The aforementioned unbalanced sediment equilibrium causes a twofold local morphological response: bed-erosion and instability of river-banks in areas where there is a sediment deficit and strong deposition and clogging in areas with a sediment excess (Kondolf, 1997). Also, from an ecological point of view, the disruption of the sediment cycle has important consequences for the riparian habitats: fine suspended sediments behave as transporting vectors of nutrients that help in algae growth (Von Bertrab et al., 2013) and also, they contribute to the creation of areas with differentiated velocity values that have a potential for fish and plants (Wood and Armitage, 1997; Kemp et al., 2011).

Furthermore, rivers channelized by man activity often display a straight path and monotonous river banks. One way to restore rivers consists of transforming the artificial banks by adding macro-roughness elements in the lateral river banks. However, these lateral cavities may be also responsible for the change of the river morphology, since they may trap the fine sediments travelling within the water.

The impact of these lateral embayments on the hydraulics of the rivers have already been thoroughly analyzed in several studies where different objectives have been targeted: (i) exchange process between the main flow and the cavity in relation to the turbulence motions in groyne fields and lateral cavities: experimental (Uijttewaal et al., 2001; Kolyshkin and Ghidaoui, 2002; Le Coz et al., 2006; Weitbrecht et al., 2001 Rivière et al., 2010; Uijttewaal, 2014; Akutina, 2015; Mignot et al., 2016) and numerical works (Hinterberger et al., 2007; McCoy et al., 2008), (ii) determination of the flow resistance effect owed to the lateral embayments created in the river banks Meile et al. (2011) and Sukhodolov (2014) and (iii) role of the sediment siltation in groynes fields for the sediment budget of rivers (Abad et al., 2008; Ten Brinke et al., 2004; Yossef and de Vriend, 2010; Henning and Hentschel, 2013). Despite the effort devoted by previous authors, laboratory experiments related to lateral embayments and morphodynamics are scarce and difficult to carry out (Henning and Hentschel, 2013) since sedimentation processes are related with: the variability of discharge, the geometrical configuration of the river banks and the sediment concentration transported in the flow. Thus far, only minimal details about measured sedimentation in laboratory channels can be found in Sukhodolov et al. (2002). Common practice, in the literature mentioned earlier, consists of deriving sedimentation patterns based on groyne field, flow patterns measured in the channels and observed in the field. However, the accuracy of the

sedimentation-erosion forecasts is hampered by the fact that the morphological response of the lateral embayment is assumed negligible in relation with the flow patterns. The fine material trapped in the embayment may modify the velocity field, enabling the alteration of the location and magnitude of the eddies and consequently, the pick-up and settling ratio of the fine particles inside the cavity.

In order to address which is the morphological answer of these lateral embayments, systematic experimental investigations in a channel have been carried out with a large number of different geometrical bank configurations. The practical questions answered in this study are: (i) which is the impact of the lateral embayments on the hydraulics patterns, (ii) which type of lateral embayment will be filled up fast with fine sediments and should be avoided in restoration projects and (iii) which type of lateral embayment will be filled up partially having zones with high and low velocities and potential for various habitat.

2 EXPERIMENTAL SETUP

2.1 Flume description

Experiments had been performed in a hydraulic system which worked in a closed circuit with different components, this included: (i) an upstream tank of 2 m long, 1 m wide and 1 m high that served as a mixing tank where suspended sediments had been mixed, (ii) a rectangular open channel which was 7.5 m long, 1.0 m wide and 1.0 m high with 0.1 % slope (typical slope for the subcritical flows in the Alpine valleys) and (iii) a downstream tank of 3.5 m long, 1 m wide and 1 m high that collected the circulating flow. The water was then pumped from down-stream to the upstream tank. A sketch of the experimental set up is shown in Figure 1.

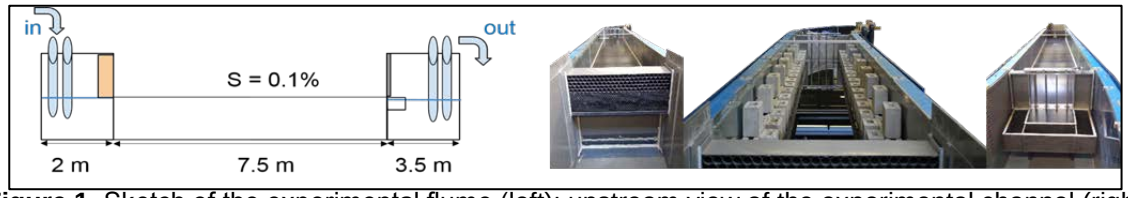

Figure 1. Sketch of the experimental flume (left); upstream view of the experimental channel (right-a); rectangular channel with the macro-roughness elements (right-b); downstream view of the experimental channel (right-c) Initial conditions.

2.2 Macro roughness configurations

The large-scale depressions, namely the rectangular cavities at the sidewalls were formed by concrete bricks (0.25 m long, 0.10 m wide, and 0.19 m high). A base channel width based on the prismatic elements, configurations 1.0, 2.0 and 3.0, had been set as a reference for all tests. They were inspired by Meile et al. (2011) who studied macro-rough flows and they were considered as large-scale depression roughness (Morris, 1955). They were characterized by the length of the cavity l, the distance between two cavities L and the lateral depth of the cavities W. These geometrical parameters had been systematically varied among them and also, in relation with the base width b of the channel as shown in Figure 2. Furthermore, the combination of the characteristics lengths of the lateral embayments led to the definition of several geometrical ratios: aspect ratio, AR= W/l, roughness ratio, RR= W/L, and expansion ratio, ER= (b+2W)/b.

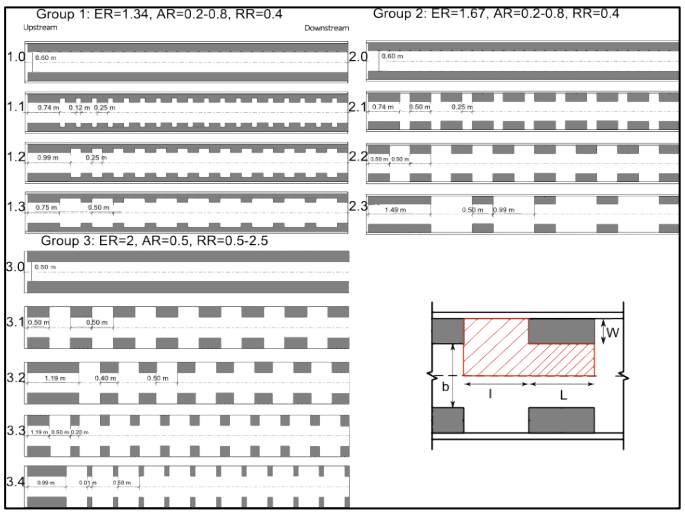

Figure 2. Geometric configurations tested and detail of the definition of the geometric lengths of the macro-roughness configurations.

The combination of these three different ratios with three different discharges had resulted in 30 different vertical axis-symmetric geometrical configurations that had been studied in this work, see Table 1.

Table 1. Summary of test ranges of the geometrical parameters of the configurations. Listed are the expansion ratio (ER), the aspect ratio (AR) and the roughness ratio (RR).

Group	Configuration	ER [-]	AR [-]	RR [-]
1	1.1	1.34	0.80	0.40
	1.2	1.34	0.40	0.40
	1.3	1.34	0.20	0.40
2	2.1	1.67	0.80	0.40
	2.2	1.67	0.40	0.40
	2.3	1.67	0.20	0.40
3	3.1	2.00	0.50	0.50
	3.2	2.00	0.50	0.60
	3.3	2.00	0.50	1.20
	3.4	2.00	0.50	2.50

2.3 Initial conditions

Three different discharges (representatives of a low, medium and peak discharge) with their corresponding maximum capacity sediment concentration had been considered in this study (Table 2). These discharges are defined by the shallowness relation b/h between the water depth, h, and the channel width, b. The influence of the water depth is well known as a key parameter: shallow flows lead to quasi-2D turbulence structures which are the net contributors for the mass exchange between the main flow and the lateral embayments (Uijttewaal et al., 2001; Uijttewaal, 2014). Conditions for the low and medium discharges allow to have shallow flows whereas the peak discharge situation is in the border of the shallowness condition.

Table 2. Summary of initial conditions for each discharge tested.

Discharge [ls^{-1}]	Q_1= 4.8	Q_2= 8.5	Q_3= 15.0
Water depth [m]	0.035	0.050	0.070
Shallowness ratio *b/h* [-]	0.26	11.50	8.20
Velocity [ms^{-1}]	0.26	0.32	0.40
Froude number [-]	0.442	0.458	0.484
Reynolds number [-]	4835	8334	13966
Concentration [gl^{-1}]	0.50	1.00	1.50
Experiment duration [h]	3.00	4.00	5.00

Characteristic values of Froude number, Reynolds number and the mean flow velocities can be seen in Table 2. These values showed that the experiments had been conducted under subcritical and turbulent conditions.

Polyurethane artificial sediments had been considered in all the experiments. The properties of this material are: a grain size of d_{50} = 0.2 mm, a density equal to 1160 kgm^{-1} and a uniformity equal to 0.47. The mean diameter of the particles was chosen to be in the range of non-cohesive fine sediment, 0.062-0.5 mm, according to Van Rijn (2007).

Sediment concentration had been chosen in order to fulfill the maximum suspended capacity of the flow. Experiments were performed until reaching a quasi-equilibrium concentration state. The channel had its own inertia regarding the sediment decay: some of the particles were trapped in the small gaps between bricks and walls. Nonetheless, the sediment concentration decay was compared with the reference situations, thus making it possible to compare it with the outcomes of all the experiments.

3 EXPERIMENTAL TECHNIQUES

3.1 2D surface PIV

The study of the flow pattern inside the cavity had been performed using a 2D-surface PIV technique as it had been previously done in (Uijttewaal et al., 2001; Weitbrecht and Jirka, 2001; Uijttewaal, 2014). Systematic photo sequences had been taken on the same cavity for the three discharges and for all the configurations. It was assumed that the position of the cavity, in the center of the channel, was representative of the flow pattern for all the cavities, as there was no influence of the channel extremities. Water-level fluctuations were also checked by means of ultrasonic probes. The accuracy of the water level measurements was at least ± 0.002 m.

The PIV technique had been applied by seeding the channel with polystyrene particles with a diameter of 3 mm and a density slightly under the one of water (0.946 gl−1). The acquisition of the photos had been done with a SUMIX SMX-160 camera, which was placed above the cavity. The recording process was performed at the beginning of the experiment at a rate of 3 frames/s (30 Hz). Photos sequences were subsequently post-processed using Matlab and the package PIVLab (Thielicke and Stamhuis, 2014): a technique of window deformation was considered to track particles in the photo sequence. The picture was divided in small interrogation areas and a cross correlation algorithm derived the most probable particle displacement. This generated an instantaneous velocity field for each time step. Next, this information was time averaged in order to analyze the stationary flow patterns present in the embayment.

The measures obtained with the surface PIV only provided information concerning the motion of the free surface. Nevertheless, the shallowness of the configurations allowed to consider that the velocity field in the embayment was mainly 2D (Tuna et al., 2013) and consequently, these results can be used as a proxy for a better comprehension of the phenomena occurring.

3.2 Suspended sediment monitoring

The temporal evolution of the suspended sediment concentration was recorded in two locations in the channel: upstream and downstream. However, a transitional length was left (close to the tranquilizer and the gate) to avoid any perturbation in the measurements.

The data acquisition was carried out by two turbidimeters Cosmos-25. The signal was sampled with a frequency of 100 ms. Subsequently, the data was averaged for every 25 time steps before storing the values of the concentration. Information provided by the turbidimeters was punctual and it corresponded to a value in the vertical concentration profile.

3.3 Sediment deposition pattern

The study of the influence of the sedimentation on the cavity was performed following a twofold protocol: (i) plan view photos of the sedimentation patterns were taken in the same cavity where the PIV technique was applied. These photos were treated for extracting the surface occupied by the sediments in order to cross-correlate their location with the information provided by the PIV technique. (ii) The total mass of sediment mass trapped inside the lateral embayments was collected. Later, the sediment samples were dried in an oven to eliminate the water content and weighted. This mass was divided by the total area occupied by the embayments in order to compute the trapping efficiency.

4 RESULTS

4.1 Flow patterns

2D surface PIV results of the lateral cavities are presented for configurations 2.2 (See Figure 3). Thanks to this technique, instantaneous (u',v') and mean velocity vectors ($\bar{u}$,$\bar{v}$) are obtained, being u and v the longitudinal and streamwise velocities respectively. Results are available for the cavity and the area of the main channel close to it. A dimensionless scale is used to characterize the cavity, x=l denotes the longitudinal direction while y=l the transversal direction. l is the length of the cavity. In addition to the velocity field, statistics on the turbulence were also performed. Mean Reynolds shear stress $\overline{u'v'}$ and mean vorticity, were computed.

Depending on the aspect ratios of the lateral embayments, the flow was characterized by the formation of one or more large-scale vortical structures that can fit the whole embayment or can occupy it partially.

For every discharge, a single clockwise recirculating system is observed. This vortex is located in the downstream part of the cavity and its center is after the 0.5 x=l position. It therefore confirms the influence of the downstream cavity wall in the reflection of the eddies: the flow hits the opposite cavity wall and the recirculating zone starts at this boundary. While the discharge is increasing, the vortex tends to be longer in the x=l direction. Regarding the velocities, a velocity plume appears when the flow leaves the cavity and it reenters in the main flow. Velocity vectors indicate that outside of the lateral embayment the flow is unidimensional following the main direction of the channel. Results indicate a clear strengthening of the vortex

velocity with discharge and it is illustrated that for the highest discharge a secondary eddy appears in bottom-left corner of the cavity.

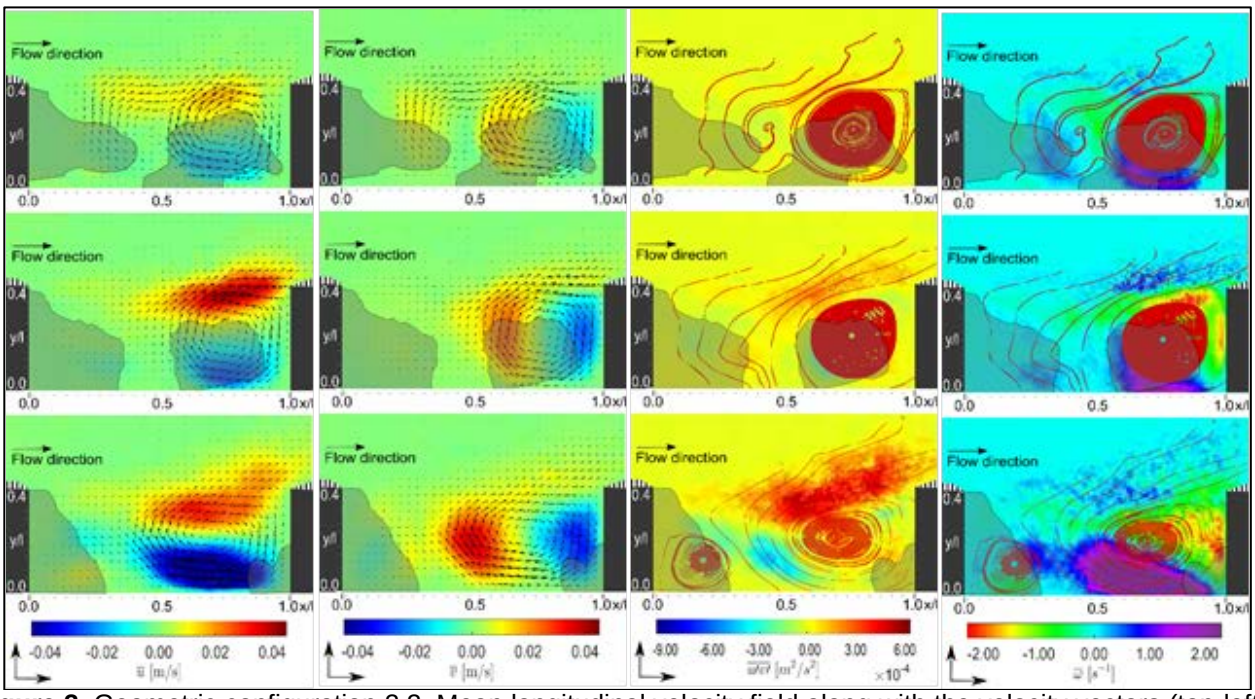

Figure 3. Geometric configuration 2.2. Mean longitudinal velocity field along with the velocity vectors (top-left); mean streamwise velocity field along with the velocity vectors (top-right); mean Reynolds shear stress field along with a few streamlines (bottom-left) and mean vorticity field along with a few streamlines (bottom-right). The results for the three different discharges are plotted from top to bottom and from 4.8 ls^{-1} to 15.0 ls^{-1}. The shaded area indicates the region where the sediments settled down at the end of the experiment. In the dashed area, the information was not available for performing the PIV computations.

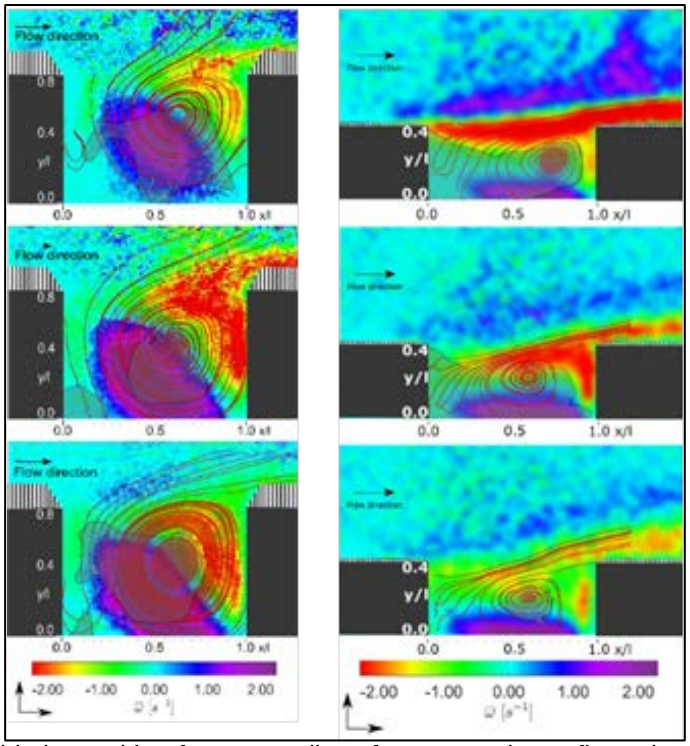

Figure 4. Mean vorticity field along with a few streamlines for geometric configuration 2.1 (left) and geometric configuration 1.3 (right). The results for the three different discharges are plotted from top to bottom and from 4.8 ls-1 to 15.0 ls-1. The shaded area indicates the region where the sediments settled down at the end of the experiment. In the dashed area, the information was not available for performing the PIV computations.

Regarding the shear stress and vorticity: two trends are observed when comparing among configurations: (i) For geometric configurations with high aspect and expansion ratios, it is stated that by increasing the discharge, the magnitude of the shear stress also increases. Thus, the vorticity also increases with higher discharges. The effect of the wall is observed in the magnitude of the vorticity which is larger in the bottom-right corner. See configuration 2.1 in Figure 4(left) as an example. (ii) However, it is observed that for configurations with low expansion and aspect ratio, higher discharges do not imply higher values of shear stress and vorticity (see configuration 1.3 in Figure 4 on the right).

4.2 Time decay of the normalized concentration

During the experiments, the concentration was continuously measured at two positions in the channel. These measurements show the dynamics of the sedimentation and although the results of the three groups show some differences, the main patterns are similar.

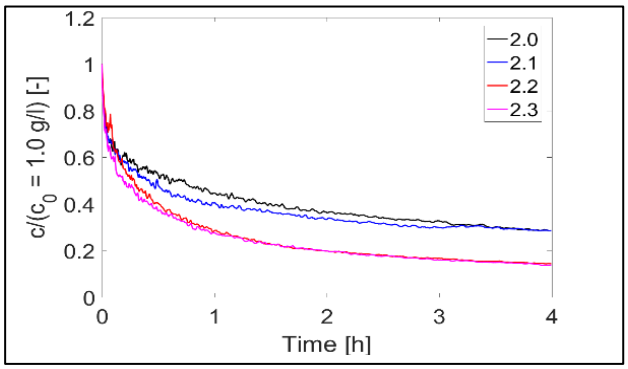

Figure 5. Geometric configurations for group 2. Time decay for the normalized sediment concentration. Results are shown for 4.8 ls-1. The curves are normalized by the initial concentration.

While the concentration of all the configurations drops rapidly in the beginning, it stabilizes and converges to an equilibrium value at the end of the experiment. Regarding the aspect ratio, one can see a correlation focusing on the dynamics. The lower the aspect ratio, the faster the drop in the concentration (see especially configuration 2.3 in Figure 5).

4.3 Trapping efficiency

To obtain the trapping efficiency of the different geometrical configurations, the trapped sediments were collected after each experiment. The total mass is then divided by the area occupied by the embayments in order to obtain the trapping efficiency. In Figure 6, these efficiencies are depicted for all the geometrical groups, starting with group 1.

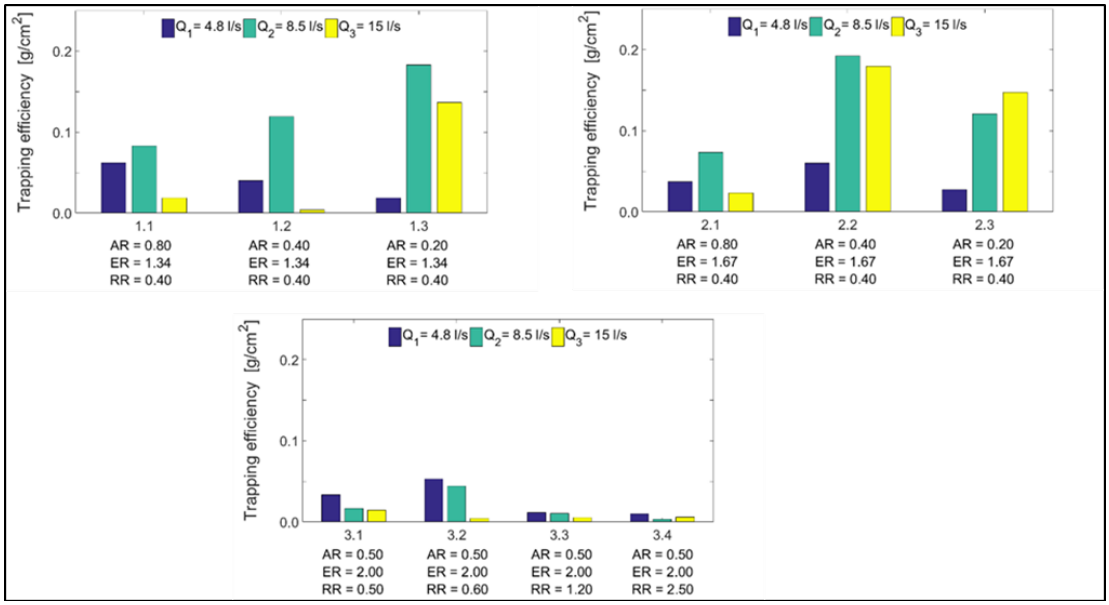

Figure 6. Trapping efficiency for all the geometric configurations. Below the figures, the values for the aspect ratio (AR), the expansion ratio (ER) and the roughness ratio (RR) are given.

Regarding the AR, it can be seen, that for the highest AR of 0.8, the lowest efficiencies are achieved. This can be observed both in groups 1 and 2. Between the smaller aspect ratios of 0.4 and 0.2, no clear tendencies are observed. There are clear tendencies regarding the discharge. The medium discharge of 8.5 ls-1 obtains the highest efficiency in all the three geometrical groups. For the low discharge, the trapping efficiency shows only small differences when changing the ratios.

5 CONCLUSIONS

The aspect ratio (AR) is the most important parameter to characterize lateral embayments. Both flow patterns and sedimentation processes are highly dependent on the AR. It is an important measure in order to analyze the location and number of eddies inside the cavities. In addition, the smaller the aspect ratio is, the more easily the flow attaches to the sidewall of the cavity. The trapping is faster and more sedimentation is trapped in the cavity.

The consequences for river restoration projects are as follows. The type of lateral embayment that will be filled up the fastest, is characterized by a small AR, a high ER and a low RR. Embayments of a larger AR and RR are providing better conditions for restoration projects, as they are not filled up as fast. This provides a more sustainable solution, as these embayments satisfy their purpose over a longer time period. In order to gain a lateral embayment that provides different zones of varying velocities and the potential for sand/ gravel banks, low AR are needed. Due to the low AR, it will be filled up partially with fine sediment inducing zones with higher and lower velocities. A combination with a rather high RR or low ER may control the sedimentation, in order to prevent completely filled up embayments.

In addition to the ratios of the embayments, the magnitude of the discharge shows a major impact on the sedimentation. The medium discharge achieves the highest trapping efficiency. The amplified gravity waves have a stabilizing effect on the shear instabilities. This causes an increased trapping efficiency for the medium discharge. For the higher discharge, the trapping is reduced, due to the intensified recirculating force of the eddies in the embayment. As the recirculation is stronger, the turbulences in the embayments are higher, which decreases the settling of the particles. Although, the exchange between the embayments and the main channel is increased for high discharges, the particles cannot settle. This can be an indicator to design artificial floods as large as possible in order to keep the small particles in motion and avoid trapping in all the low flow areas downstream.

The flow pattern recorded by the PIV shows a good correlation with the observed sedimentation patterns. The main vortex corresponds generally well to the area of sediment deposition in the embayment. Further, a coherent mixing layer is also found. And, high positive velocities correspond to areas that are free of sedimentation. However, for cavities of higher ER some inconsistencies can be seen. They can be explained by the three-dimensional conditions in this wide shallow embayments.

ACKNOWLEDGEMENTS

This work was funded by the ITN-Programme (Marie Curie Actions) of the European Union's Seventh Framework Programme FP7-PEOPLE-2013-ITN under REA grant agreement 607394-SEDITRANS. The experiments were funded by FOEN (Federal Office for the Environment, Switzerland).

REFERENCES

Abad, J., Rhoads, B., Guneralp, I. & Garcia, M. (2008). Flow Structure at Different Stages in Ameander-Bend with Bendway Weirs. *Journal of Hydraulic Research*, 134(8), 1052-1063.

Akutina, Y. (2015). Experimental Investigation of Flow Structures in a Shallow Embayment using 3D-PTV, *PhD Thesis*. McGill University, Montréal.

Allan, J.D. & Castillo, M.M. (2007). *Stream Ecology: Structure and Function of Running Waters*. Springer, Netherlands.

Henning, M. & Hentschel, B. (2013). Sedimentation and Flow Patterns Induced by Regular and Modified Groynes on the River Elbe, Germany. *Ecohydrology*, 6(4), 598-610.

Hinterberger, C., Frohlich, J. & Rodi, W. (2007). Threedimensional and Depth-Averaged Large Eddy Simulations of Some Shallow Water Flows. *Journal of Hydraulic Engineering*, 133(8), 857-872.

Kemp, P., Sear, D., Collins, A., Naden, P. & Jones, I.(2011). The Impacts of Ne Sediment on Riverine Fish. *Hydrological Processes*, 25, 1800-1821.

Kolyshkin, A.A. & Ghidaoui, M.S. (2002). Gravitational Shear Instabilities in Compound and Composite Channels. *Journal of Hydraulic Engineering*, 128(12), 1076-1086.

Kondolf, G.M. (1997). Hungry Water: Effects of Dams and Gravel Mining on River Channels. *Environnemental Management*, 21(4), 533-551.

Le Coz, J., Brevis, W. & Niño, Y. (2006). Open-Channel Side-Cavities: A Comparison of Field and Flume Experiments. In River Flow 2006, Two Volume Set: *Proceedings of the International Conference on Fluvial Hydraulics, Lisbon*, Portugal, 6-8 September 2006 (145). CRC Press.

McCartney, M. (2009). Living with Dams: Managing the Environmental Impacts. *Water Policy,* 11(S1), 121-139.

Constantinescu, G. & Weber, L.J. (2008). Numerical Investigation of Ow Hydrodynamics in a Channel with a Series of Groynes. *Journal of Hydraulic Engineering*, 134(2), 157-172.

Meile, T., Boillat, J.-L. & Schleiss, A.J. (2011). Flow Resistance Caused by Large-Scale Bank Roughness in a Channel. *Journal of Hydraulic Engineering*, 137(12), 1588-1597.

Mignot, E., Cai, W., Launay, G., Rivière, N. & Escauriaza C. (2016). Coherent Turbulent Structures at the Mixing-Interface of a Square Open-Channel Lateral Cavity. *Physics of Fluids*, 28(4), 045104.

Morris, M.H. (1955). A New Concept of Flow in Rough Conduits. *Transactions American Society of Civil Engineers*, 120, 373-410.

Rivière, N., Garcia, M., Mignot, E. & Travin, G. (2010). Characteristics of the Recirculation Cell Pattern in a Lateral Cavity. *Proc. Int. Conf. Fluvial Hydraul., IAHR*, 673-679.

Schleiss, A.J., Franca, M.J., Juez, C. & De Cesare, G. (2016). Reservoir Sedimentation, *Journal of Hydraulic Research,* 54(6), 595–614.

Sukhodolov, A (2014). Hydrodynamics of Groyne Fields in A Straight River Reach: Insight from Field Experiments. *Journal of Hydraulic Research*, 52(1), 105-120.

Ten Brinke, W.B.M., Schulze, F. & Van Der Veer, P (2004). Sand Exchange between Groyne-Field Beaches and The Navigation Channel of The Dutch Rhine: The Impact of Navigation Versus River Flow. *River Research and Applications*, 20, 899-928.

Thielicke, W. & Stamhuis, E.J. (2014). PIVlab – Towards User-friendly, Affordable and Accurate Digital Particle Image Velocimetry in MATLAB. Journal *Open Research Software*, 2(1), 1-30.

Tuna, B., Tinar, E. & Rockwell, D.(2013). Shallow Ow Past A Cavity: Globally Coupled Oscillations as a Function of Depth. *Experiments and Fluids*, 54(8), 1586.

Uijttewaal, W.S.J. (2014). Hydrodynamics of Shallow Flows: Application to Rivers. *Journal of Hydraulic Research,* 52, 157–172.

Uijttewaal, W.S.J., Lehmann, D.V. & Mazijk, A.V. (2001). Exchange Processes between a River and Its Groyne Fields: Model Experiments. *Journal of Hydraulic Engineering*, 127(11), 928-936.

Von Bertrab, M.G., Krein, A., Stendera, S., Thielen, F. & Hering,D. (2013). Is Fine Sediment Deposition a Main Driver for The Composition of Benthic Macroinvertebrate Assemblages? *Ecological Indicators*, 24, 589-598.

Van Rijn, L.C.(2007). Unified View of Sediment Transport by Currents and Waves. I: Initiation of Motion, Bed Roughness, and Bed-Load Transport. *Journal of Hydraulic Engineering*, 133, 649–667.

Weitbrecht, V. & Jirka, G.H.(2001). Flow Patterns and Exchange Processes in Dead Zones of Rivers, in: *Proceedings of the Congress-International Association for Hydraulic Research*. 439–445.

Wood, P.J. & Armitage, P.D. (1997). Biological Effects of Fine Sediment in the Lotic Environment. *Environnemental Management*, 21, 203–217.

Yossef, M.F.M. & de Vriend, H.J. (2010). Sediment Exchange between A River and its Groyne Fields: Mobile-Bed Experiment. *Journal of Hydraulic Engineering*, 136, 610–625.

